







Research Article

A New Statistical Approach Based on the Access of Electricity Application with Some Modified Control Charts

Riffat Jabeen ¹, Mashhood Ahmad ¹, Azam Zaka ², Mahmoud M. Mansour ^{3,4},
Abdussalam Aljadani ⁵ and Enayat M. Abd Elrazik ^{3,4}

¹Department of Statistics, COMSATS University Islamabad, Lahore Campus, Lahore, Pakistan

²Department of Statistics, Government Graduate College of Science, Wahdat Road, Lahore, Pakistan

³Department of Management Information Systems, Taibah University, Yanbu 46422, Saudi Arabia

⁴Department of Statistics, Mathematics, and Insurance, Benha University, Benha 13511, Egypt

⁵Department of Management, College of Business Administration in Yanbu, Taibah University, Al-Madinah Al-Munawarah 41411, Saudi Arabia

Correspondence should be addressed to Riffat Jabeen; riffat.jabeen79@gmail.com

Received 12 July 2023; Revised 24 March 2024; Accepted 24 April 2024; Published 4 May 2024

Academic Editor: Çetin Yildiz

Copyright © 2024 Riffat Jabeen et al. This is an open access article distributed under the Creative Commons Attribution License, which permits unrestricted use, distribution, and reproduction in any medium, provided the original work is properly cited.

This article introduces a new probability model based on reflected parameter called the reflected Pareto (RP) distribution. The key properties of the RP model are investigated. A simulation study of the RP model is conducted to evaluate the performances of its estimators. A real-life application is considered to examine the performance of proposed model. The different criteria are discussed numerically as well as graphically to show the flexibility of the RP model. The exponential weighted moving average control charts based on the maximum likelihood and modified maximum likelihood estimators for the shape parameter of the RP distribution are obtained. Detailed simulation results of proposed charts are performed to examine and analyze the performance of these charts with three in-control average run length values and two sample sizes. Finally, the application of the proposed control charts is shown by considering a real-life data set.

1. Introduction

The applications of Pareto distribution have been discussed in various applied fields such as actuarial science, medical science, and engineering. The estimation methods for the parameters of the Pareto distribution is discussed in [1]. The estimation of the shape and scale parameters of the Pareto model are obtained through the maximum likelihood (ML) and moment estimations approaches [1]. The comparison between estimation methods of the Pareto parameters is addressed in [2]. The classical and Bayesian estimation for Pareto distribution is reported in [3]. Some basic methods for estimation of parameters of the generalized Pareto distribution are addressed by [4]. Evaluation of various generalized Pareto probability distributions for flood frequency analysis are discussed in [5].

Several techniques have been used in the literature to propose new forms of the Pareto model by adding additional

parameters for generating new efficient and flexible Pareto models. For example, the Pareto alpha-power Pareto (APP) [6], inverse Pareto (IP) [7], new Kumaraswamy-Pareto (NKP) [8], beta-Pareto (BP) [9], exponentiated Weibull-Pareto [10], among others.

In this paper, a new Pareto distribution is introduced called the reflected Pareto (RP) distribution. The application of RP model is reported on the access of electricity data. We addressed its properties. The proposed model is compared with some competing models based on goodness-of-fit measures including the Kolmogorov-Smirnov (KS) test, its p value, Akaike information criteria (AIC), Bayesian information criteria (BIC), consistent Akaike information criteria (CAIC), and Hannan-Quinn information criteria (HQIC) to verify its superiority. The estimation of the shape parameter of the RP distribution is conducted using the ML and modified ML (MML) estimators. Some new modified

control charts based on the RP model such as exponential weighted moving average (EWMA) control charts. Visual presentation of the EWMA control charts is presented in both usual and 3D plots.

The new EWMA control chart for monitoring multinomial proportions is suggested in [11]. The Shewhart and EWMA control charts for monitoring the shape parameter of reflected power function distribution are studied in [12]. The are proposed. The comparison of modified Shewhart, EWMA, and HEWMA control charts using Monte Carlo simulation and real-life applications are presented [13].

This article is arranged in the following sections. In Section 2, the identification of the proposed model is introduced. In Section 3, properties of the RP model are discussed. Estimation of the RP parameters and a simulation study are presented in Section 4. Section 5 provides a real-life data application. The newly proposed control charts are explored in Section 6. The conclusion of this study is discussed in Section 7.

2. Model Identification

The probability density function (PDF) of the Pareto distribution has the form

$$f(y) = \frac{\alpha\beta^\alpha}{y^{\alpha+1}}, \quad y \geq \beta \text{ or } \beta \leq y \leq \infty, \quad (1)$$

where α and β are shape and scale parameters respectively.

The cumulative distribution function (CDF) of Pareto distribution reduces to

$$F(y) = 1 - \left(\frac{\beta}{y}\right)^\alpha. \quad (2)$$

If θ is a reflected parameter, then by setting $y = \theta - x$, in the PDF of Pareto distribution (1), we obtain the PDF of the RP distribution as follows:

$$f(x) = \frac{\alpha\beta^\alpha}{(\theta-x)^{\alpha+1}}, \quad -\infty < x < \theta - \beta, \alpha, \beta, \theta \geq 0. \quad (3)$$

The CDF of the RP distribution reduces to

$$F(x) = \frac{\beta^\alpha}{(\theta-x)^\alpha}. \quad (4)$$

The survival function (SF) and hazard rate function (HRF) of the RP distribution are given by

$$S(x) = 1 - \frac{\beta^\alpha}{(\theta-x)^\alpha}, \quad (5)$$

$$h(x) = \frac{\alpha\beta^\alpha(\theta-x)^\alpha}{(\theta-x)^{\alpha+1}[(\theta-x)^\alpha - \beta^\alpha]}.$$

2.1. Asymptotic Behavior of RP Distribution. In this section, some asymptotic behavior of the RP distribution relevant to PDF, CDF, SF, and HRF are given by

$$(i) \lim_{x \rightarrow 0} f(x) = \infty; \text{ if } \theta = 0, \alpha, \beta, \geq 1$$

$$(ii) \lim_{x \rightarrow \infty} f(x) = 0; \forall \alpha, \beta, \theta$$

$$(iii) \lim_{x \rightarrow 0} F(x) = \infty; \text{ if } \theta = 0, \alpha, \beta, \geq 1$$

$$(iv) \lim_{x \rightarrow \infty} F(x) = 0; \quad \forall \alpha, \beta, \theta$$

$$(v) \lim_{x \rightarrow 0} S(x) = 1; \text{ if } \beta = \theta$$

$$(vi) \lim_{x \rightarrow \infty} S(x) = 0; \text{ if } \alpha = 0$$

$$(vii) \lim_{x \rightarrow 0} h(x) = 0; \text{ if } \alpha = 0, \forall \beta, \theta$$

$$(viii) \lim_{x \rightarrow \infty} h(x) = 0; \text{ if } \alpha = 0, \forall \beta, \theta$$

2.2. Special Cases. In this section, some special cases of the RP distribution are addressed.

(1) By setting $x = \theta - y$ in the PDF of the RP distribution, we get the Pareto distribution.

$$f(y) = \frac{\alpha\beta^\alpha}{y^{\alpha+1}}. \quad (6)$$

(2) Setting $x = \theta - y$ in the RP density and multiply it by $y^{2\alpha}/\beta^{2\alpha}$, gives PDF of the power function distribution.

$$f(y) = \frac{\alpha y^{\alpha-1}}{\beta^\alpha}. \quad (7)$$

Figure 1 provides the probability distribution loop plot. In Figure 2, the plots show that the RP distribution is reflected image of the Pareto (P) distribution. Figure 3 gives the plots for the CDF and HRF of the RP distribution. The HRF of the RP model is always increasing.

3. Properties

This section presents some properties of RP distribution.

3.1. Moments. The r th moments of the RP distribution follows as

$$E(x^r) = \alpha\beta^\alpha\theta^{-\alpha} \left[\frac{(-1)^r \theta^r \Gamma(1+r)\Gamma(-r+\theta)}{\Gamma(1+\alpha)} + \frac{(\theta-\beta)^{2+r}}{(1+r)\theta} \sum_{j=0}^{\infty} \frac{(1+r)_j (1+\alpha)_j}{(2+r)_j} \frac{(1-\beta/\theta)^j}{j!} \right]. \quad (8)$$

3.2. Quantile Function. The quantile function (QF) of the RP distribution has the following form:

$$x_p = \theta - \frac{\beta}{(p)^{1/\alpha}}, \quad 0 < p < 1. \quad (9)$$

Note that x_p can be used to generate random variates from the RP model.

3.3. Order Statistics. Let X_1, X_2, \dots, X_n denotes a random sample of size n and $X_{(1)}, X_{(2)}, \dots, X_{(n)}$ denote the order statistics. The PDF of j th order statistic, $X_{(j)}$, is obtained as

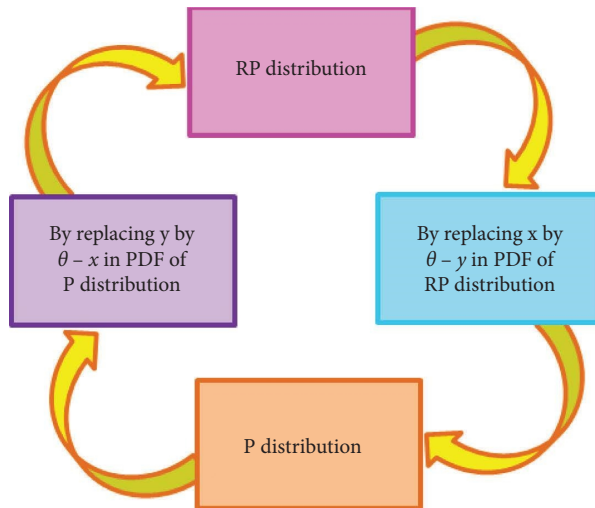


FIGURE 1: Probability distribution loop plot.

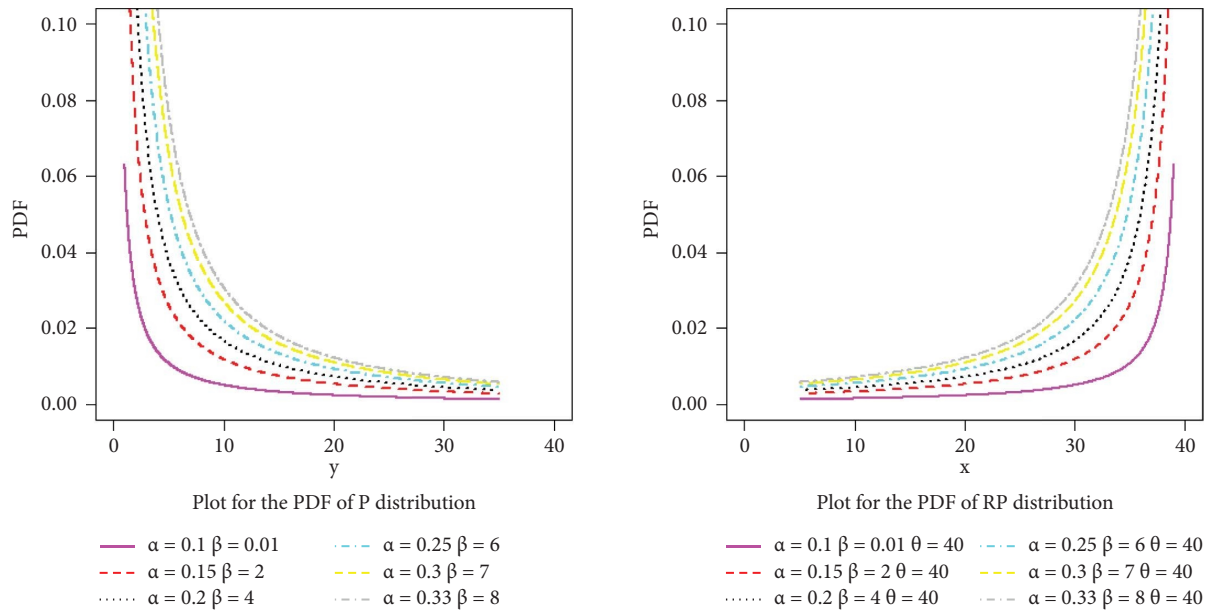


FIGURE 2: Plots for the PDF of the P and RP distributions.

$$f_{X_{(j)}}(x) = \frac{n!}{(j-1)!(n-j)!} [f(x)][F(x)]^{j-1} [1-F(x)]^{n-j}. \quad (10)$$

Then, the PDF of j th order statistic $X_{(j)}$ of the RP distribution follows as

$$f_{X_{(j)}}(x) = \frac{n!}{(j-1)!(n-j)!} \left[\frac{\alpha\beta^\alpha}{(\theta-x)^{\alpha+1}} \right] \left[\frac{\beta^\alpha}{(\theta-x)^\alpha} \right]^{j-1} \left[1 - \frac{\beta^\alpha}{(\theta-x)^\alpha} \right]^{n-j}. \quad (11)$$

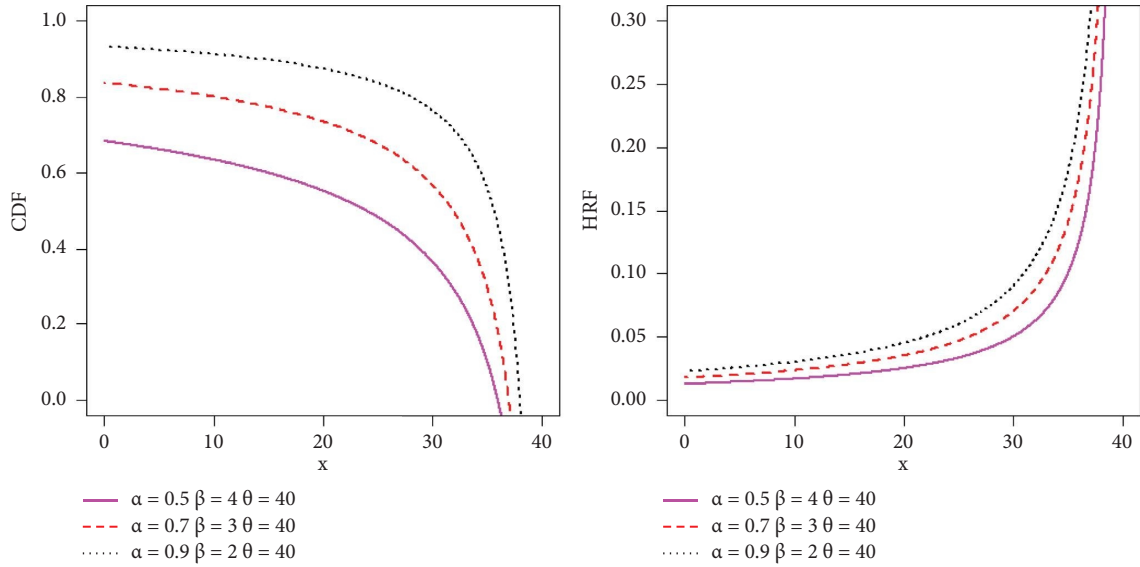


FIGURE 3: Plots for the CDF and HRF of the RP distribution.

The PDF of largest order statistic $X_{(n)}$ of the RP distribution is obtained as follows:

$$f_{X_{(n)}}(x) = n \left[\frac{\alpha\beta^\alpha}{(\theta-x)^{\alpha+1}} \right] \left[\frac{\beta^\alpha}{(\theta-x)^\alpha} \right]^{n-1}. \quad (12)$$

The PDF of smallest order statistics $X_{(1)}$ of the RP distribution reduces to

$$f_{X_{(1)}}(x) = n \left[\frac{\alpha\beta^\alpha}{(\theta-x)^{\alpha+1}} \right] \left[1 - \frac{\beta^\alpha}{(\theta-x)^\alpha} \right]^{n-1}. \quad (13)$$

4. Estimation of Parameters

The parameters of the RP distribution are estimated by two estimation techniques called the maximum likelihood (ML) and modified ML (MML) estimation.

4.1. *Maximum Likelihood.* The ML estimator (MLE) of the RP parameter follows as

$$L(\alpha, \beta) = \prod_{i=1}^n \frac{\alpha\beta^\alpha}{(\theta-x_i)^{\alpha+1}}. \quad (14)$$

The MLE of the parameter α takes the form

$$\hat{\alpha}_{MLE} = \frac{n}{\sum_{i=1}^n \ln(\theta-x_i) - n \ln \hat{\beta}}. \quad (15)$$

As when took partial derivative w.r.t to β , it does not exist so likelihood function is maximize by taking $\hat{\beta}_{MLE} = x_n$ where x_n is maximum value in the data.

4.2. *Modified Maximum Likelihood.* The MML estimators (MMLEs) of the RP parameters are given by

$$\begin{aligned} \hat{\beta}_{MMLE} &= (\theta - \bar{x})(0.5)^{1/\alpha}, \\ \hat{\alpha}_{MMLE} &= \frac{n}{\sum_{i=1}^n \ln(\theta-x_i) - n \ln(\theta - \bar{x})(0.5)^{1/\alpha}}. \end{aligned} \quad (16)$$

4.3. *Simulation Study.* The three combinations of the RP distribution parameters used to compare the two estimation methods, numerically based on simulation results. The results are reported for the three samples sizes $n=100, 200,$ and 400 . The R software is used to obtain the simulation results based on the following steps.

- (1) Random values are obtained from the RP distribution for three sample sizes and two methods of estimation.
- (2) Step 1 is repeated $N=5000$ times. The RP parameters are estimated for each parameter combination and each sample, using two estimators including the MML, MMLE.
- (3) The average values (Avg) and mean square errors (MSE) of estimates are obtained for each parameter combination with each sample.

The results are reported in Table 1. These results show that both estimation methods achieved the consistency property, i.e., the MSE decrease as n increases, for all parameter combinations.

5. Real Life Application

In this section, the RP model is fitted using a real-life data set to show its flexibility in modeling real data as compared to other models.

TABLE 1: The Avg and MSE of different estimators of the RP parameters with $\theta = 2$.

Methods	n	Parameters		Avg of estimates		MSE	
		α	β	Avg ($\hat{\alpha}$)	Avg ($\hat{\beta}$)	MSE ($\hat{\alpha}$)	MSE ($\hat{\beta}$)
MLE	100	1.9	1.8	0.3610	0.1905	2.3688	2.5905
	200			0.3640	0.1952	2.3592	2.5754
	400			0.3657	0.1976	2.3542	2.5676
	100	1.8	1.9	0.2764	0.0892	2.3215	3.2792
	200			0.2814	0.0948	2.3063	3.2588
	400			0.2835	0.0974	2.2996	3.2494
	100	2.1	1.7	0.4467	0.2917	2.7334	1.9832
	200			0.4497	0.2960	2.7236	1.9713
	400			0.4510	0.2979	2.7193	1.9658
	MMLE	100	1.9	1.8	2.2368	1.8085	0.1489
200		2.2219			1.8037	0.1215	0.0047
400		2.2152			1.8012	0.1080	0.0023
100		1.8	1.9	2.0242	1.9091	0.0769	0.0120
200				2.0136	1.9036	0.0591	0.0055
400				2.0118	1.9030	0.0517	0.0029
100		2.1	1.7	2.6075	1.7046	0.3084	0.0066
200				2.5934	1.7036	0.2699	0.0034
400				2.5830	1.7010	0.2464	0.0016

The real data set is available online through the link: . The data refer to “Access to electricity (% of population).” “Access to electricity is the percentage of population with access to electricity. Electrification data are collected from industry, national surveys and international sources.” The data is available for many countries in that file. The data of country “Tunisia” is selected for this study and the data values are: 86.8, 88.7, 90.4, 92, 93.2, 94.2, 94.80000305, 97.30000305, 97.80000305, 98.40000153, 99, 99.30000305, 99.40000153, 99.40000153, 99.40000153, 99.5, 99.5, 99.5, 99.5, 99.69999695, 99.80000305, 99.90000153, 100, 100, 99.80000305, 100, 100.

The proposed model is compared with new Weibull-Pareto (NWP) [14], exponentiated Pareto (EP) [15] and tapered Pareto (TP) [16] distributions. These models are compared with each other on the bases of some goodness-of-fit measures including the Kolmogorov-Smirnov (KS) test, its p -value (KS p -value), Akaike information criteria (AIC), Hannan-Quinn information criteria (HQIC), Bayesian information criteria (BIC), and consistent AIC (CAIC).

Table 2 reports the MLEs of the parameters of the fitted distributions along with the above-mentioned measures for the analyzed real data. The numerical values in this table illustrate that the proposed RP model provides a better fit as compared to competing models.

The box, Q-Q, TTT and KDE plots are given in Figure 4. The estimated PDF, estimated CDF, estimated HRF and PP plots of the RP model are given in Figure 5. The 3D plots of the estimated PDF and HRF for the data are reported in Figure 6. The visual comparison based on the AIC, BIC, CAIC, and HQIC measures are displayed in Figure 7. These plots supports the results in Table 2.

6. EWMA Control Chart

6.1. EWMA Control Chart Based on the MLE. The EWMA statistics at time t is given by

$$Z_{(t)} = \lambda X_{(t)} + (1 - \lambda)Z_{(t-1)}, \tag{17}$$

where λ is a weighting constant, whose values lies between 0 and 1 ($0 < \lambda \leq 1$).

Now, the MLE of shape parameter $\hat{\alpha}_{MLE(t)}$ of the RP distribution used instead of using variable $X_{(t)}$, i.e $X_{(t)} = \hat{\alpha}_{MLE(t)}$.

Hence, $Z_{(t)} = \lambda \hat{\alpha}_{MLE(t)} + (1 - \lambda)Z_{(t-1)}$, where $Z_{(t)}$ is the EWMA statistic on current time and $Z_{(t-1)}$ is EWMA statistic on previous time.

The EWMA control limits based on the MLE are obtained as

$$UCL_{Z(t)} = \alpha + L \sqrt{Var(\hat{\alpha}_{MLE}) \left[\frac{\lambda}{2 - \lambda} \right] [1 - (1 - \lambda)^{2t}]},$$

$$CL_{Z(t)} = \alpha, \tag{18}$$

$$LCL_{Z(t)} = \alpha - L \sqrt{Var(\hat{\alpha}_{MLE}) \left[\frac{\lambda}{2 - \lambda} \right] [1 - (1 - \lambda)^{2t}]}.$$

The remaining term after ignoring the term $[1 - (1 - \lambda)^{2t}]$ are given by

$$UCL_{Z(t)} = \alpha + L \sqrt{Var(\hat{\alpha}_{MLE}) \left[\frac{\lambda}{2 - \lambda} \right]},$$

$$CL_{Z(t)} = \alpha, \tag{19}$$

$$LCL_{Z(t)} = \alpha - L \sqrt{Var(\hat{\alpha}_{MLE}) \left[\frac{\lambda}{2 - \lambda} \right]}.$$

TABLE 2: The MLEs, KS, p value, AIC, BIC, CAIC and HQIC for real data.

Model	MLEs	KS	KS p value	AIC	BIC	CAIC	HQIC	$-\log(\hat{\theta})$
RP	1.9509 104.0001 3.5999	0.187	0.301	118.459	122.347	119.502	119.615	56.229
NWP	43.3155 108.1888 51.1459	0.3053	0.013	141.228	145.115	142.271	142.384	67.614
EP	23.5278 104.8216 53.8774	0.313	0.010	142.508	146.396	143.552	143.664	68.254
TP	2.65937 84.2161 20.1693	0.384	0.0006	200.177	204.064	201.221	201.333	97.0885

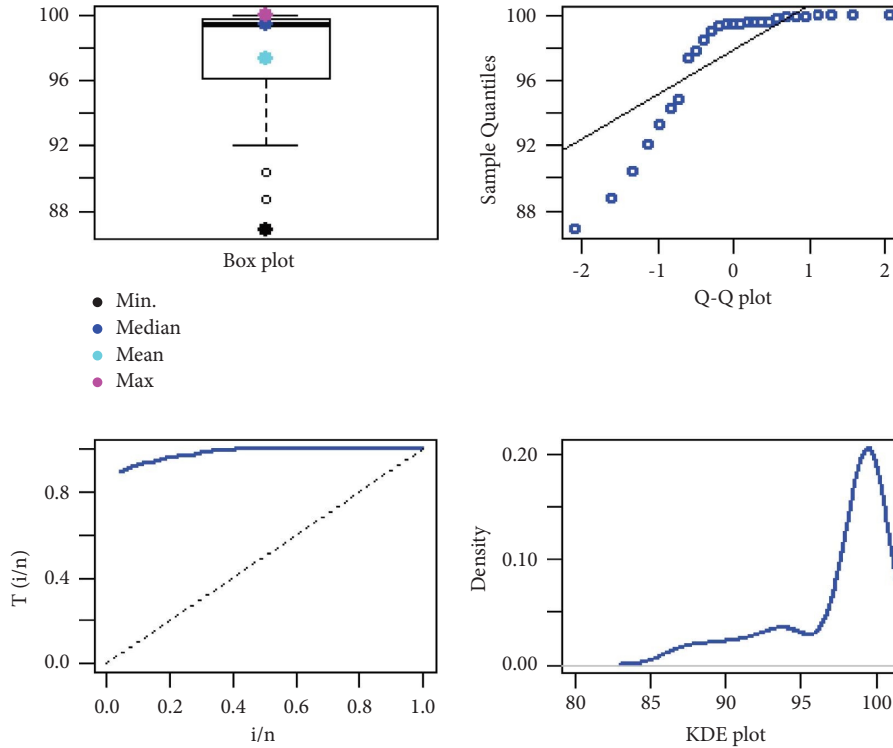


FIGURE 4: Box plot, Q-Q plot, TTT plot and KDE plot for the data.

The random values are generated with $n = 500$ from the RP distribution, with parameters $(\alpha, \beta, \theta, \lambda) = (1.5, 1.8, 3, 0.1)$ as displayed in Figure 8. The obtained $\hat{\alpha}_{MLE}$ are computed from the random values. Repeated this step for 30 times and computed $Var(\hat{\alpha}_{MLE})$. The control limits of the EWMA control charts based on $\hat{\alpha}_{MLE}$ are computed from the above obtained results and plotted $Z_{(t)}$ against the sample (subgroup).

6.2. EWMA Control Chart Based on MMLE. The EWMA statistic at time t is given by

$$Z_{(t)} = \lambda X_{(t)} + (1 - \lambda)Z_{(t-1)}, \tag{20}$$

where λ is a weighting constant, whose values lies between 0 and 1 ($0 < \lambda \leq 1$).

Here, the MMLE of shape parameter $\hat{\alpha}_{MMLE(t)}$ of the RP distribution used instead of using variable $X_{(t)}$, i.e $X_{(t)} = \hat{\alpha}_{MMLE(t)}$.

$Z_{(t)} = \lambda \hat{\alpha}_{MMLE(t)} + (1 - \lambda)Z_{(t-1)}$, where $Z_{(t)}$ is the EWMA statistics on current time and $Z_{(t-1)}$ is the EWMA statistics on previous time.

The EWMA control limits based on MMLE are obtained as follows:

$$\begin{aligned}
 UCL_{Z_{(t)}} &= \alpha + L \sqrt{Var(\hat{\alpha}_{MMLE}) \left[\frac{\lambda}{2 - \lambda} \right] [1 - (1 - \lambda)^{2t}]}, \\
 CL_{Z_{(t)}} &= \alpha, \\
 LCL_{Z_{(t)}} &= \alpha - L \sqrt{Var(\hat{\alpha}_{MMLE}) \left[\frac{\lambda}{2 - \lambda} \right] [1 - (1 - \lambda)^{2t}]},
 \end{aligned} \tag{21}$$

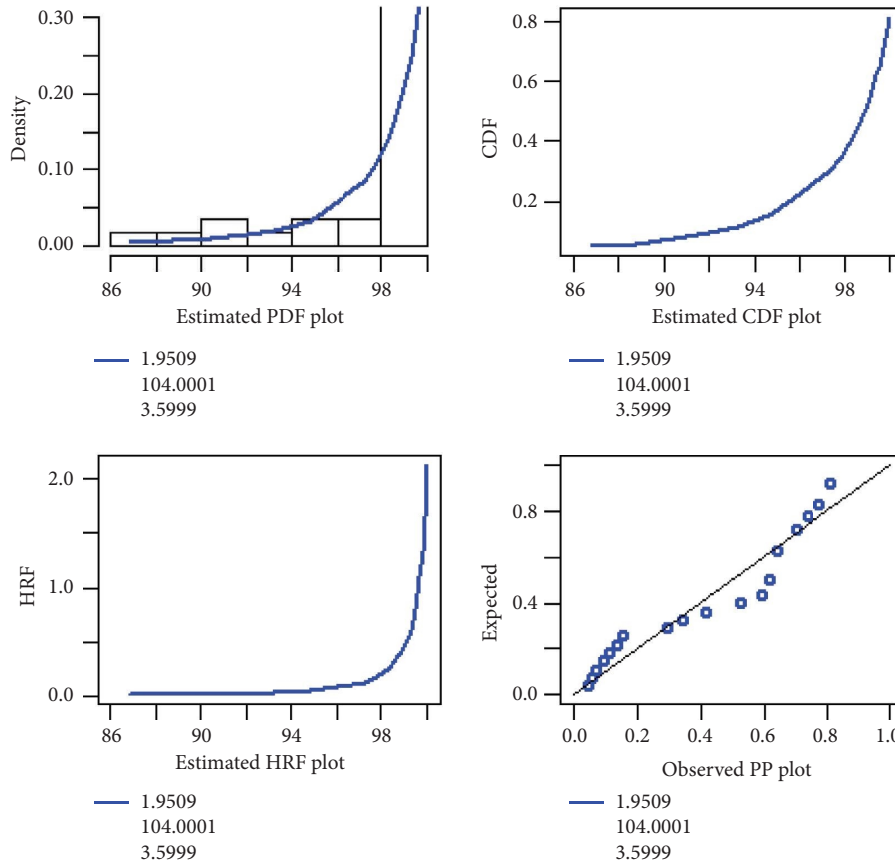


FIGURE 5: The estimated PDF, CDF, HRF and PP plots of the RP model for the data.

The remaining term after ignoring the term $[1 - (1 - \lambda)^{2t}]$ are given as follows:

$$\begin{aligned}
 UCL_{Z(t)} &= \alpha + L \sqrt{\text{Var}(\hat{\alpha}_{MMLE}) \left[\frac{\lambda}{2 - \lambda} \right]}, \\
 CL_{Z(t)} &= \alpha, \\
 LCL_{Z(t)} &= \alpha - L \sqrt{\text{Var}(\hat{\alpha}_{MMLE}) \left[\frac{\lambda}{2 - \lambda} \right]}.
 \end{aligned}
 \tag{22}$$

The random values are generated with $n = 500$ from the RP distribution with parameter values $(\alpha, \beta, \theta, \lambda) = (3, 1, 2, 0.25)$ as given in Figure 9. Then, $\hat{\alpha}_{MMLE}$ is obtained by computing the random values. Repeated this step for 30 times and computed $\text{Var}(\hat{\alpha}_{MMLE})$. The control limits of the EWMA control charts based on $\hat{\alpha}_{MMLE}$ are computed from the above obtained results and plotted $Z_{(t)}$ against the sample (subgroup).

6.3. Simultaneous Study. For checking the performance of the EWMA control chart based on $\hat{\alpha}_*$, a Monte Carlo simulation study is performed, where * = MLE or MMLE. Simulations are performed based on the following steps.

- (1) The random values are generated with $n = 200$ from the RP distribution, with parameters $(\alpha, \beta, \theta, \lambda) = (1.6, 2.3, 4.7, 0.92)$.

- (2) The estimate $\hat{\alpha}_*$ are computed from the random values that obtained in step 1.
- (3) For both types of estimators, the above two steps are repeated 2000 times and $\text{Var}(\hat{\alpha}_*)$ is computed.
- (4) The control limits of the EWMA control charts based on $\hat{\alpha}_*$ are computed from the results obtained in 3rd step.
- (5) The $ARL_0 = 370$ is fixed for in-control state of the process and found that value of L at which $ARL_0 = 370$ for in-control state for both type of estimator. Same procedure is repeated for $ARL_0 = 300$ and $ARL_0 = 200$.
- (6) The different shifts i.e., shifts = 0, 3.05, 3.1, 3.2, 3.4, 3.6, 3.8, 4, 4.2, 4.4, 4.6 are used and the ARL_1 is computed against the values of shifts for both types of estimators.
- (7) The values of $SDRL, P_{10}, P_{30}, P_{50}, P_{70}, P_{90}$ are also reported.
- (8) All above steps are repeated for $n = 100$.

In Tables 3–8 and Figures 10–15, the comparison of the $ARL_{(\alpha_{MLE})}$ and $ARL_{(\alpha_{MMLE})}$ are obtained. By using the $ARL_0 = 370, 300, 200$ it is noted that the $ARL_{(\alpha_{MMLE})}$ provided a smaller ARL_1 as compared to the $ARL_{(\alpha_{MLE})}$ for all shifts.

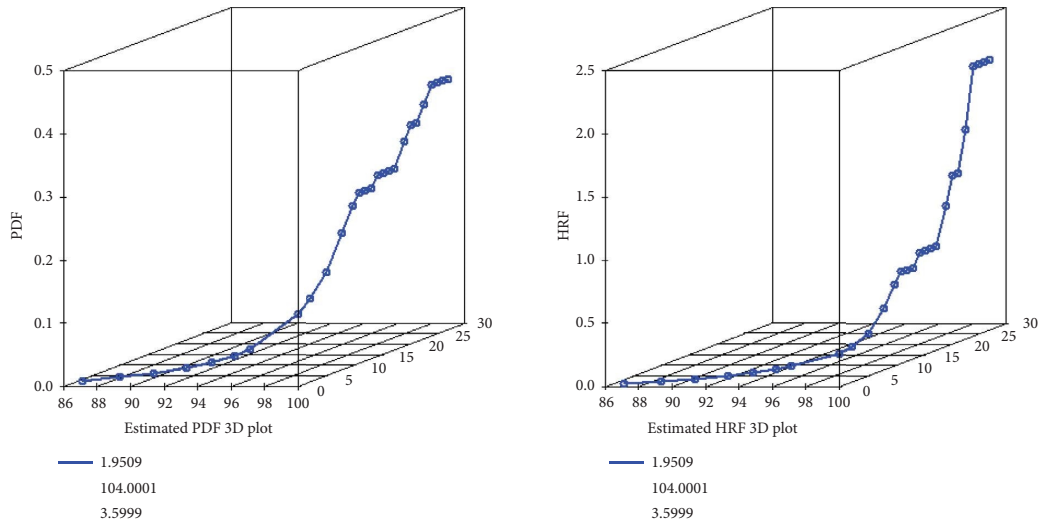


FIGURE 6: The plots of the estimated PDF and HRF for the data.

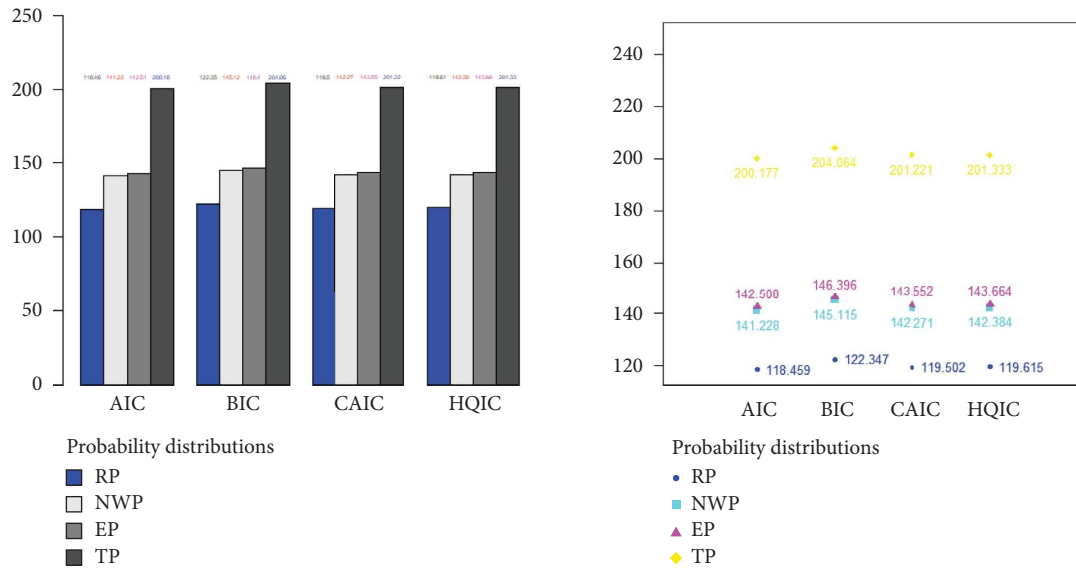


FIGURE 7: Visual comparison between the fitted models.

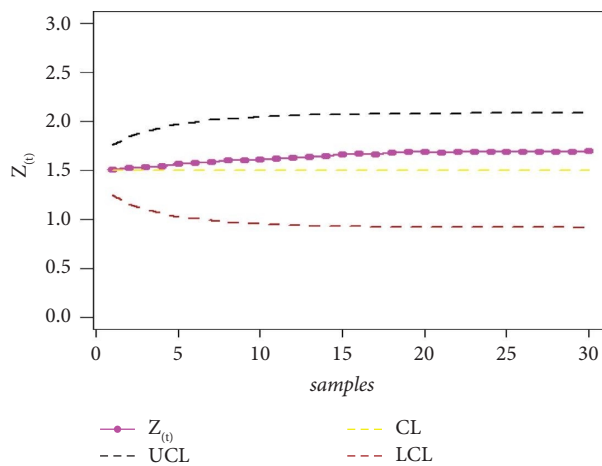


FIGURE 8: The EWMA control chart based on the MLE.

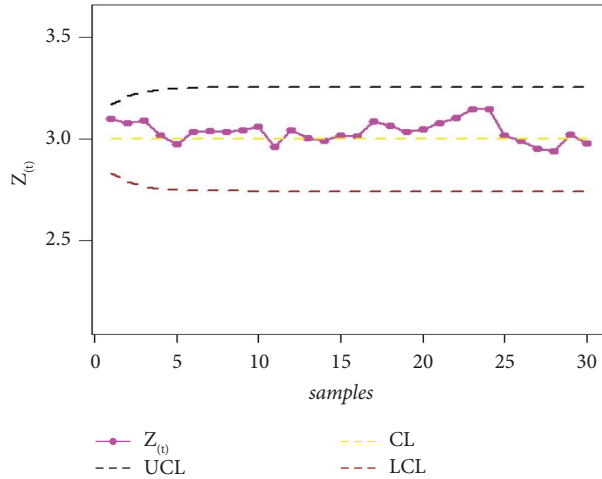


FIGURE 9: The EWMA control chart based on MMLE.

TABLE 3: Comparison of the $ARL_{(\alpha_{MLE})}$ and $ARL_{(\alpha_{MMLE})}$ when $ARL_{0(\alpha_{MLE})} = ARL_{0(\alpha_{MMLE})} = 370$ by using the EWMA control charts with $n = 200$.

Methods	Shifts	ARL	SDRL	P_{10}	P_{30}	P_{50}	P_{70}	P_{90}
MLE	0	370.7605	345.6954	38	145	269.5	457	846.1
	3.05	93.779	90.54939	10	35	66	114	214.1
	3.1	80.6275	79.8897	8	28.7	55.5	99	192.1
	3.2	57.957	56.3122	7	23	42	68	132
	3.4	33.1595	31.81401	4	12	23	41	75
	3.6	19.0685	18.47862	3	7	13	24	42
	3.8	12.4265	11.68139	2	5	9	15	28
	4	8.189	7.953924	1	3	6	10	18.1
	4.2	5.7065	5.359545	1	2	4	7	13
	4.4	4.2545	3.961133	1	2	3	5	9
4.6	3.184	2.736401	1	1	2	4	7	
MMLE	0	370.666	359.6461	35	129	265.5	451.3	856.4
	2.5	1.6835	1.10993	1	1	1	2	3
	3.1	1.6525	1.086892	1	1	1	2	3
	3.2	1.5835	0.951042	1	1	1	2	3
	3.4	1.4025	0.75085	1	1	1	1	2
	3.6	1.3025	0.645137	1	1	1	1	2
	3.8	1.2205	0.546836	1	1	1	1	2
	4	1.1365	0.391081	1	1	1	1	2
	4.2	1.1085	0.350413	1	1	1	1	1
	4.4	1.06	0.251857	1	1	1	1	1
4.6	1.0535	0.235936	1	1	1	1	1	

TABLE 4: Comparison of the $ARL_{(\alpha_{MLE})}$ and $ARL_{(\alpha_{MMLE})}$ when $ARL_{0(\alpha_{MLE})} = ARL_{0(\alpha_{MMLE})} = 370$ by using the EWMA control charts with $n = 100$.

Methods	Shifts	ARL	SDRL	P_{10}	P_{30}	P_{50}	P_{70}	P_{90}
MLE	0	370.21	361.8405	39	128	254	454.6	889.3
	2.5	43.8005	42.78773	5	16	31	54	101
	3.1	38.4295	38.852	4	14	27	46	87
	3.2	28.168	28.55776	3	10	20	33	63
	3.4	17.0265	16.57206	2	6	12	21	38
	3.6	10.8385	10.2469	1	4	8	13	24
	3.8	7.2875	6.797569	1	3	5	9	16
	4	5.1535	4.82012	1	2	4	6	11
	4.2	3.908	3.418242	1	2	3	5	8
	4.4	2.968	2.531834	1	1	2	3	6
4.6	2.4395	1.964248	1	1	2	3	5	

TABLE 4: Continued.

Methods	Shifts	ARL	SDRL	P_{10}	P_{30}	P_{50}	P_{70}	P_{90}
MMLE	0	370.873	346.3069	39	135	270	450	857
	2.5	1.775	1.17135	1	1	1	2	3
	3.1	1.69	1.156533	1	1	1	2	3
	3.2	1.616	1.076161	1	1	1	2	3
	3.4	1.45	0.844901	1	1	1	2	2
	3.6	1.3195	0.666815	1	1	1	1	2
	3.8	1.2245	0.523676	1	1	1	1	2
	4	1.1655	0.445207	1	1	1	1	2
	4.2	1.1115	0.355149	1	1	1	1	1
	4.4	1.082	0.307121	1	1	1	1	1
	4.6	1.0555	0.249902	1	1	1	1	1

TABLE 5: Comparison of the $ARL_{(\alpha_{MLE})}$ and $ARL_{(\alpha_{MMLE})}$ when $ARL_{0(\alpha_{MLE})} = ARL_{0(\alpha_{MMLE})} = 300$ by using the EWMA control charts with $n = 200$.

Methods	Shifts	ARL	SDRL	P_{10}	P_{30}	P_{50}	P_{70}	P_{90}
MLE	0	300.671	292.3798	32	111	210.5	369.3	701.4
	3.05	67.3875	66.62309	7	26	47	80	155.1
	3.1	55.5485	54.39414	6	20	38	67	129
	3.2	42.8245	42.40573	5	14	30	52	100
	3.4	24.75	24.25493	3	9	17	29	57
	3.6	15.174	15.34531	2	6	10	18	34
	3.8	10.0275	9.719001	1	4	7	12	23
	4	6.722	6.40728	1	3	5	8	15
	4.2	5.0665	4.511125	1	2	4	6	11
	4.4	3.542	3.130037	1	1	3	4	8
	4.6	2.8505	2.235542	1	1	2	3	6
MMLE	0	300.4515	299.5582	30.9	107	206.5	360.3	693.1
	2.5	1.629	1.03629	1	1	1	2	3
	3.1	1.563	0.918397	1	1	1	2	3
	3.2	1.483	0.888316	1	1	1	2	3
	3.4	1.371	0.72844	1	1	1	1	2
	3.6	1.253	0.582375	1	1	1	1	2
	3.8	1.181	0.486166	1	1	1	1	2
	4	1.1255	0.380555	1	1	1	1	2
	4.2	1.0945	0.345875	1	1	1	1	1
	4.4	1.0575	0.245406	1	1	1	1	1
	4.6	1.038	0.206343	1	1	1	1	1

TABLE 6: Comparison of the $ARL_{(\alpha_{MLE})}$ and $ARL_{(\alpha_{MMLE})}$ when $ARL_{0(\alpha_{MLE})} = ARL_{0(\alpha_{MMLE})} = 300$ by using the EWMA control charts with $n = 100$.

Methods	Shifts	ARL	SDRL	P_{10}	P_{30}	P_{50}	P_{70}	P_{90}
MLE	0	300.193	301.5449	31	100	205	355.3	719.5
	3.05	32.849	33.87167	4	12	23	38	76
	3.1	28.986	28.88993	4	11	20	34	65
	3.2	21.1835	20.59726	3	8	15	25	48
	3.4	13.197	12.8232	2	5	9	15	30
	3.6	8.569	8.194377	1	3	6	10	19
	3.8	6.0215	5.70897	1	2	4	7	13
	4	4.401	3.925163	1	2	3	5	10
	4.2	3.459	2.938475	1	1	3	4	7
	4.4	2.7215	2.25754	1	1	2	3	6
	4.6	2.2955	1.788793	1	1	2	3	5

TABLE 6: Continued.

Methods	Shifts	ARL	SDRL	P_{10}	P_{30}	P_{50}	P_{70}	P_{90}
MMLE	0	300.2065	294.8528	32	106	204	362	714.3
	2.5	1.6965	1.123841	1	1	1	2	3
	3.1	1.6095	1.021534	1	1	1	2	3
	3.2	1.525	0.926177	1	1	1	2	3
	3.4	1.4185	0.79792	1	1	1	1	2
	3.6	1.2705	0.592879	1	1	1	1	2
	3.8	1.231	0.564622	1	1	1	1	2
	4	1.1455	0.423579	1	1	1	1	2
	4.2	1.106	0.334395	1	1	1	1	1
	4.4	1.0635	0.251991	1	1	1	1	1
	4.6	1.0455	0.220123	1	1	1	1	1

TABLE 7: Comparison of the $ARL_{(\alpha_{MLE})}$ and $ARL_{(\alpha_{MMLE})}$ when $ARL_{0(\alpha_{MLE})} = ARL_{0(\alpha_{MMLE})} = 200$ by using the EWMA control charts with $n = 200$.

Methods	Shifts	ARL	SDRL	P_{10}	P_{30}	P_{50}	P_{70}	P_{90}
MLE	0	200.367	198.1372	22.9	70	141	245	466.2
	3.05	37.7055	37.42263	4	14	27	45	86
	3.1	33.03	31.90847	4	12	23	40	72.1
	3.2	26.1705	26.39126	3	9	18	31	61
	3.4	15.2635	14.66512	2	6	11	18	35
	3.6	10.083	9.665703	1	4	7	12	23
	3.8	7.1215	7.006374	1	3	5	8	16
	4	4.99	4.716887	1	2	4	6	11
	4.2	3.6355	3.16317	1	1	3	4	8
	4.4	2.9295	2.433617	1	1	2	3	6
	4.6	2.3615	1.892249	1	1	2	3	5
MMLE	0	200.367	193.8012	21	72.7	139	246	462.1
	2.5	1.5	0.917835	1	1	1	2	3
	3.1	1.4725	0.866383	1	1	1	2	3
	3.2	1.3995	0.772138	1	1	1	1	2
	3.4	1.2715	0.599973	1	1	1	1	2
	3.6	1.187	0.476597	1	1	1	1	2
	3.8	1.143	0.40575	1	1	1	1	2
	4	1.097	0.338598	1	1	1	1	1
	4.2	1.0645	0.26339	1	1	1	1	1
	4.4	1.0435	0.213613	1	1	1	1	1
	4.6	1.028	0.17097	1	1	1	1	1

TABLE 8: Comparison of the $ARL_{(\alpha_{MLE})}$ and $ARL_{(\alpha_{MMLE})}$ when $ARL_{0(\alpha_{MLE})} = ARL_{0(\alpha_{MMLE})} = 200$ by using the EWMA control charts with $n = 100$.

Methods	Shifts	ARL	SDRL	P_{10}	P_{30}	P_{50}	P_{70}	P_{90}
MLE	0	200.16	203.1541	20	67	133	241	472.3
	3.05	17.7035	17.11707	2	7	13	21	40
	3.1	16.176	15.82451	2	6	11	19	38
	3.2	12.7665	12.65631	2	5	9	15	30
	3.4	8.414	8.080857	1	3	6	10	18
	3.6	5.9335	5.406819	1	2	4	7	13
	3.8	4.3285	3.860057	1	2	3	5	10
	4	3.3525	2.903008	1	1	2	4	7
	4.2	2.6075	2.216958	1	1	2	3	5
	4.4	2.2005	1.661228	1	1	2	2	4
	4.6	1.835	1.273808	1	1	1	2	4

TABLE 8: Continued.

Methods	Shifts	ARL	SDRL	P_{10}	P_{30}	P_{50}	P_{70}	P_{90}
MMLE	0	200.542	198.8219	21	73.7	139.5	240.3	450.5
	2.5	1.5635	0.943617	1	1	1	2	3
	3.1	1.5345	0.932333	1	1	1	2	3
	3.2	1.451	0.833634	1	1	1	2	3
	3.4	1.2935	0.665266	1	1	1	1	2
	3.6	1.2135	0.532033	1	1	1	1	2
	3.8	1.1645	0.459941	1	1	1	1	2
	4	1.103	0.344166	1	1	1	1	1
	4.2	1.0825	0.296205	1	1	1	1	1
	4.4	1.0455	0.21553	1	1	1	1	1
4.6	1.039	0.208568	1	1	1	1	1	

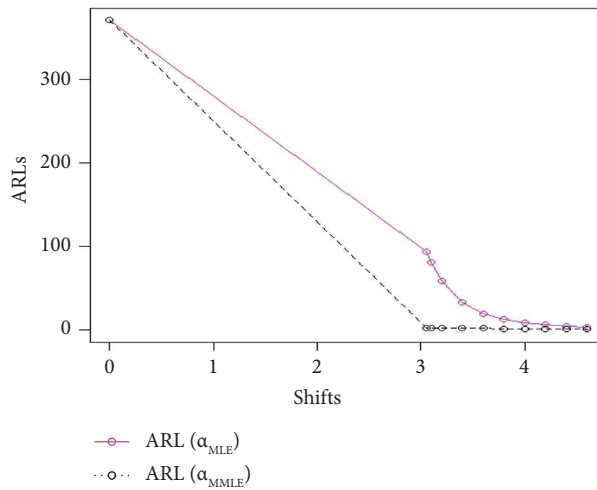


FIGURE 10: Comparison of the $ARL_{(\alpha_{MLE})}$ and $ARL_{(\alpha_{MMLE})}$ when $ARL_{0(\alpha_{MLE})} = ARL_{0(\alpha_{MMLE})} = 370$ by using the EWMA control charts with $n = 200$.

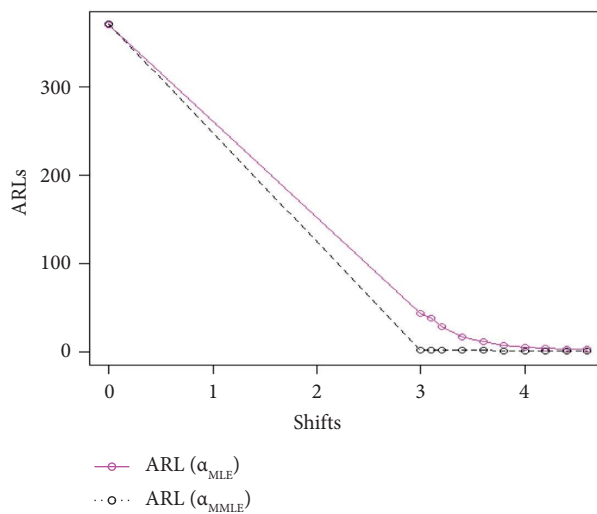


FIGURE 11: Comparison of the $ARL_{(\alpha_{MLE})}$ and $ARL_{(\alpha_{MMLE})}$ when $ARL_{0(\alpha_{MLE})} = ARL_{0(\alpha_{MMLE})} = 370$ by using the EWMA control charts with $n = 100$.

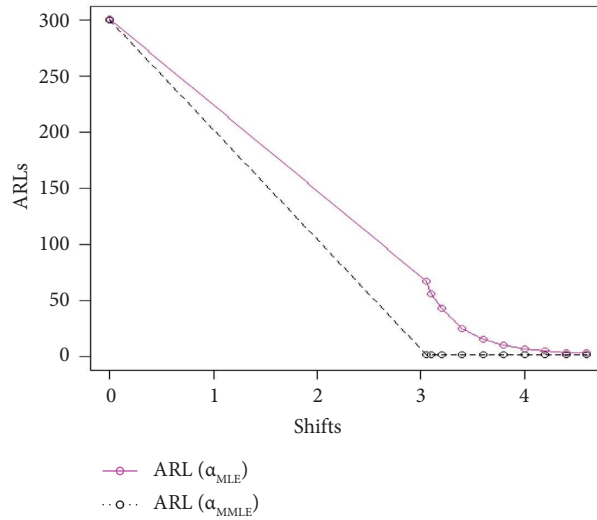


FIGURE 12: Comparison of the $ARL_{(\alpha_{MLE})}$ and $ARL_{(\alpha_{MMLE})}$ when $ARL_{0(\alpha_{MLE})} = ARL_{0(\alpha_{MMLE})} = 300$ by using the EWMA control charts with $n = 200$.

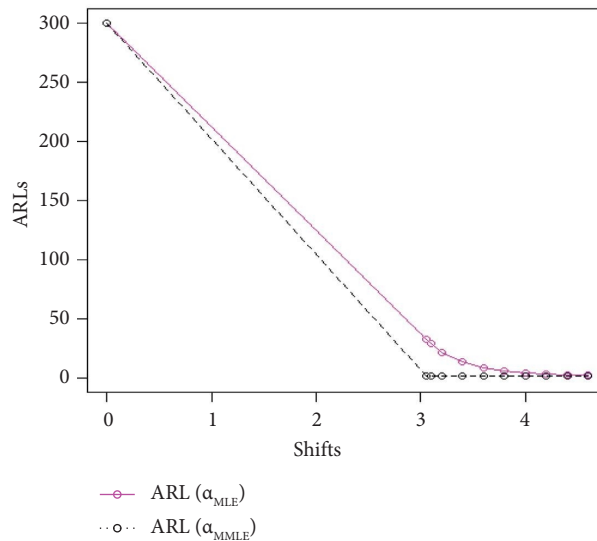


FIGURE 13: Comparison of the $ARL_{(\alpha_{MLE})}$ and $ARL_{(\alpha_{MMLE})}$ when $ARL_{0(\alpha_{MLE})} = ARL_{0(\alpha_{MMLE})} = 300$ by using the EWMA control charts with $n = 100$.

6.4. Application of the EWMA Control Charts. A data set is adopted from Tables 9 and 10 in [17] and the proposed EWMA control charts by using the MLE and MMLE. The results are listed in Tables 9 and 10. The results also are displayed visually in Figures 15 and 16.

The simulated results of EWMA control chart based on the MLE from real data are reported in Table 9 and Figure 15.

The simulated results of the EWMA control chart based on the MMLE from real data are reported in Table 10 and Figures 16 and 17.

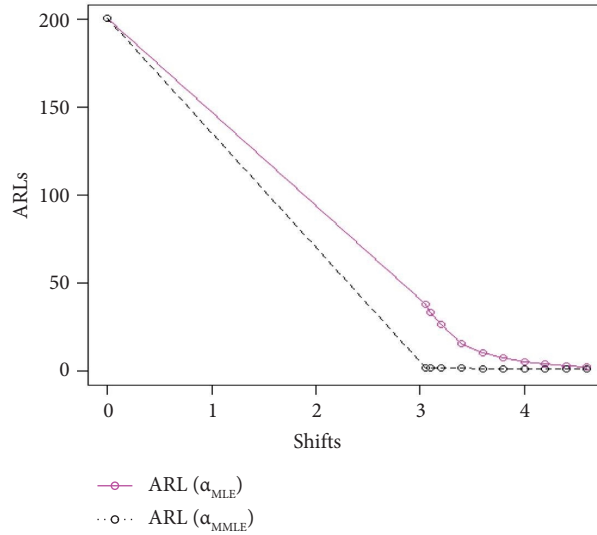


FIGURE 14: Comparison of the $ARL_{(\alpha_{MLE})}$ and $ARL_{(\alpha_{MMLE})}$ when $ARL_{0(\alpha_{MLE})} = ARL_{0(\alpha_{MMLE})} = 200$ by using the EWMA control charts with $n = 200$.

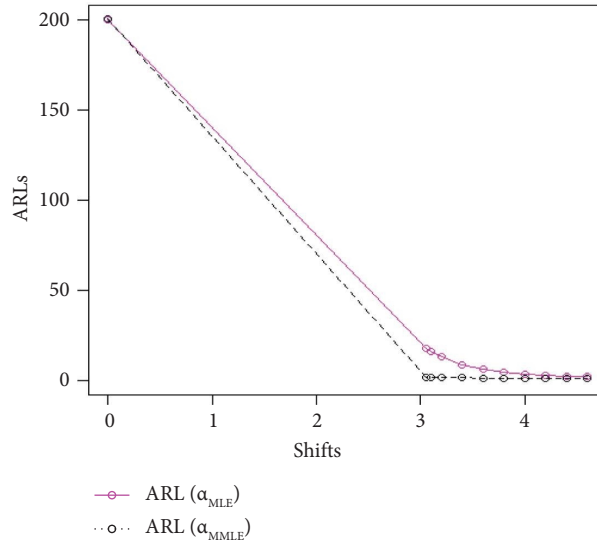


FIGURE 15: Comparison of the $ARL_{(\alpha_{MLE})}$ and $ARL_{(\alpha_{MMLE})}$ when $ARL_{0(\alpha_{MLE})} = ARL_{0(\alpha_{MMLE})} = 200$ by using the EWMA control charts with $n = 100$.

TABLE 9: Simulated results of the EWMA control chart based on the MLE from real data.

Serial no	Subgroups (i)	x_i	Z	EWMA by using MLE	
				UCL	LCL
1	1	9.45	1.907597	1.976067	1.823933
2	2	7.99	1.91049	2.007038	1.792962
3	3	9.29	1.917361	2.030443	1.769557
4	4	11.66	1.939393	2.049876	1.750124
5	5	12.16	1.967641	2.066739	1.733261
6	6	10.18	1.977915	2.081755	1.718245
7	7	8.04	1.980231	2.095355	1.704645
8	8	11.46	1.999566	2.107823	1.692177
9	9	9.2	2.005212	2.119356	1.680644
10	10	10.34	2.015984	2.130099	1.669901
11	11	9.03	2.020861	2.140163	1.659837
12	12	11.47	2.039888	2.149632	1.650368
13	13	10.51	2.05131	2.158578	1.641422
14	14	9.4	2.057196	2.167054	1.632946
15	15	10.08	2.066057	2.175109	1.624891

TABLE 10: Simulated results of the EWMA control chart based on the MMLE from real data.

Serial no	Subgroups (i)	x_i	EWMA by using MMLE		
			Z	UCL	LCL
1	1	9.45	1.901503	1.920534	1.879466
2	2	7.99	1.900126	1.928895	1.871105
3	3	9.29	1.901256	1.935213	1.864787
4	4	11.66	1.910456	1.94046	1.85954
5	5	12.16	1.922439	1.945012	1.854988
6	6	10.18	1.925654	1.949065	1.850935
7	7	8.04	1.924117	1.952737	1.847263
8	8	11.46	1.932104	1.956102	1.843898
9	9	9.2	1.932712	1.959216	1.840784
10	10	10.34	1.936312	1.962116	1.837884
11	11	9.03	1.936511	1.964833	1.835167
12	12	11.47	1.944421	1.967389	1.832611
13	13	10.51	1.94845	1.969804	1.830196
14	14	9.4	1.94935	1.972092	1.827908
15	15	10.08	1.952004	1.974267	1.825733

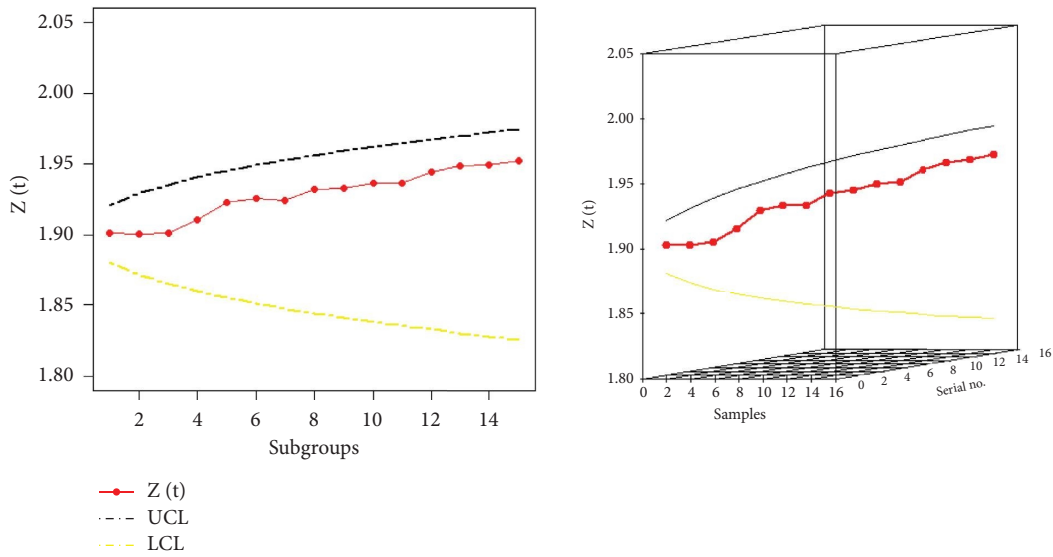


FIGURE 16: Simulated results of EWMA control chart based on MMLE from real data.

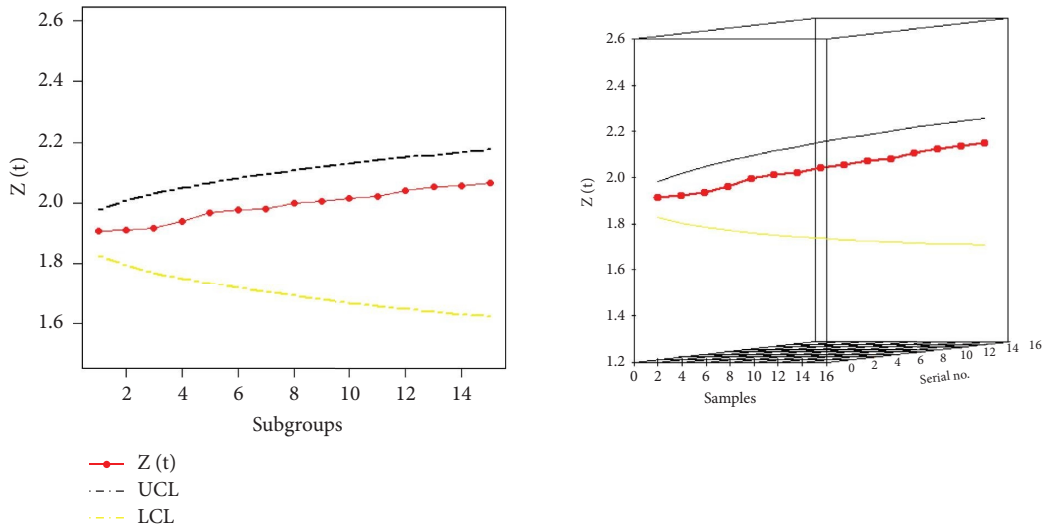


FIGURE 17: Simulated results of the EWMA control chart based on MLE from real data.

7. Conclusions

A new probabilistic model is introduced by adding a new parameter to the Pareto distribution called the reflected Pareto (RP) distribution. Some properties of the RP distribution are discussed. Moreover, the RP distribution parameters are estimated by using two estimation methods. The performance of the two methods is explored through simulations. A real-life data set is fitted using the RP model to prove its superiority as compared to some competing models. Additionally, the EWMA control chart based on the maximum likelihood and modified maximum likelihood estimators are discussed in detail. Finally, simulations and real-life data analysis are discussed to validate the results of the EWMA control chart.

Data Availability

The data used to support the findings of this study are included in the article.

Conflicts of Interest

The authors declare that they have no conflicts of interest to report regarding the present study.

Acknowledgments

The authors extend their appreciation to the Deputyship for Research and Innovation, Ministry of Education in Saudi Arabia for funding this research work through project number 445-9-916.

References

- [1] M. Rytgaard, "Estimation in the pareto distribution," *Astin Bulletin*, vol. 20, no. 2, pp. 201–216, 1990.
- [2] Warsono, E. Gustavia, D. Kurniasari, Amanto, and Y. Antonio, "On the comparison of the methods of parameter estimation for Pareto distribution," *Journal of Physics: Conference Series*, vol. 1338, no. 1, Article ID 012042, 2019.
- [3] A. S. Hassan, E. A. Elsherpieny, and R. E. Mohamed, "Classical and Bayesian estimation of entropy for Pareto distribution in presence of outliers with application," *Sankhya Services*, vol. 86, 2022.
- [4] J. Martín, M. I. Parra, M. M. Pizarro, and E. L. Sanjuán, "Baseline methods for the parameter estimation of the generalized Pareto distribution," *Entropy*, vol. 24, no. 2, p. 178, 2022.
- [5] C. G. Anghel and C. Ilinca, "Evaluation of various generalized pareto probability distributions for flood frequency analysis," *Water*, vol. 15, no. 8, p. 1557, 2023.
- [6] S. Ihtisham, A. Khalil, S. Manzoor, S. A. Khan, and A. Ali, "Alpha-power Pareto distribution: its properties and applications," *PLoS One*, vol. 14, no. 6, Article ID e0218027, 2019.
- [7] S. Dankunprasert, U. Jaroengertakun, and T. Talangtam, "The properties of inverse Pareto distribution and its application to extreme events," *Thailand Statistian*, vol. 19, pp. 1–13, 2021.
- [8] M. Ahmad, R. Jabeen, A. Zaka, W. A. Hamdi, and B. Alnssyan, "A unified generalized family of distributions: properties, inference, and real-life applications," *AIP Advances*, vol. 14, no. 1, Article ID 015043, 2024.
- [9] B. Boumaraf, N. Seddik-Ameur, and V. S. Barbu, "Estimation of beta-Pareto Distribution based on several optimization methods," *Mathematics*, vol. 8, no. 7, p. 1055, 2020.
- [10] A. Z. Afify, H. M. Yousof, G. G. Hamedani, and G. R. Aryal, "The exponentiated Weibull-Pareto distribution with application," *Journal of Statistical Theory and Applications*, vol. 15, no. 4, pp. 326–344, 2016.
- [11] S. Gan, S. Yang, and L. P. Chen, "A new EWMA control chart for monitoring multinomial proportions," *Sustainability*, vol. 15, Article ID 11797, 2023.
- [12] A. Zaka, A. Saeed Akhter, and R. Jabeen, "The new reflected power function distribution: theory, simulation and application," *AIMS Mathematics*, vol. 5, pp. 5031–5054, 2020.
- [13] R. Jabeen and A. Zaka, "The modified control charts for monitoring the shape parameter of weighted power function distribution under classical estimator," *Quality and Reliability Engineering International*, vol. 37, no. 8, pp. 3417–3430, 2021.
- [14] S. Nasiru and A. Luguterah, "The new Weibull-Pareto distribution," *Pakistan Journal of Statistics and Operation Research*, vol. 11, no. 1, pp. 103–114, 2015.
- [15] A. I. Shawky and H. H. Abu-Zinadah, "Exponentiated Pareto distribution: different method of estimations," *International Journal of Contemporary Mathematical Sciences*, vol. 4, no. 15, pp. 677–693, 2009.
- [16] Y. Y. Kagan and F. Schoenberg, "Estimation of the upper cutoff parameter for the tapered Pareto distribution," *Journal of Applied Probability*, vol. 38, pp. 158–175, 2001.
- [17] D. Montgomery, *Introduction to Statistical Quality Control*, John Wiley and Sons, Inc, New York, NY, USA, 2009.